Journal of Environmental Chemical Engineering 10 (2022) 108231

Contents lists available at ScienceDirect

Journal of Environmental Chemical Engineering

journal homepage: www.elsevier.com/locate/jece

# Photocatalytic activation of peroxymonosulfate using ilmenite ($FeTiO_3$) for *Enterococcus faecalis* inactivation

Patricia García-Muñoz [a,*], Cecilia López-Maxías [a], Sonia Guerra-Rodríguez [a], Jaime Carbajo [b], Jose A. Casas [b], Jorge Rodríguez-Chueca [a,*]

[a] Universidad Politécnica de Madrid (UPM), E.T.S de Ingenieros Industriales, Departamento de Ingeniería Química Industrial y del Medio Ambiente, c/José Gutiérrez Abascal 2, 28006 Madrid, Spain

[b] Sección departamental de Ingeniería Química, Facultad de Ciencias, Universidad Autónoma de Madrid, 28049 Madrid, Spain

ARTICLE INFO

Editor: T.T. Lim

*Keywords:*
Wastewater reuse
Disinfection
*Enterococcus faecalis*
Advanced oxidation processes
Peroxymonosulfate
Ilmenite
UV-A radiation

ABSTRACT

In this work, a raw and low cost mineral, ilmenite ($FeTiO_3$), has been tested for the first time as a photocatalyst paired with peroxymonosulfate ($HSO_5^-$; PMS) for the inactivation of *Enterococcus faecalis* as an alternative to conventional treatments to disinfect wastewater for reuse. The influence of some operational parameters such as reagent dosage, catalyst concentration, initial pH, or flow rate was also studied and optimized. After several tests, the scarce pure photoactivity under UV-A was remarked by ilmenite because of its high iron content, which favors photogenerated charge recombination. However, ilmenite activity was highly promoted when combined with low concentrations of PMS and UV-A light, reaching total inactivation of *Enterococcus faecalis* in 120 min. Quenching tests were performed using methanol, *tert*-butyl alcohol, furfuryl alcohol, and Cu(II) to assess the main reactive species involved in the disinfection process determining the critical role of both HO·and $SO_4^{\cdot-}$ radicals in the process. Finally, the influence of the water matrix was also evaluated by studying the effect of water hardness and the presence of nutrients on the system. Overall, the PMS/Ilmenite/UV-A system yielded promising results with a total removal of *Enterococcus faecalis* in 120 min. However, it also showed the need for further study and understanding of the disinfection mechanism to achieve the same level of performance in real wastewater.

## 1. Introduction

Today, the presence of bacteria, viruses, and other microorganisms transmitted by water remains a global public health problem as one of the main sources of mortality in the world [1,2]. In a recent report of the WHO (2019) [3], it is estimated that fecal polluted water can kill 829, 000 people per year, including 485,000 deaths associated with diseases caused by drinking water pollution containing rotavirus and *Escherichia coli*. Taking this into account, a large proportion of these diseases could be prevented only through a safe water supply. So far, there has been an increasing need to control microbial contamination in water for human health. This is mainly the case in low- and middle-income countries, while in developed countries the threat of fecal pollution could come from the risks associated with the reuse of treated wastewater [4–6], as well as the presence of other pollutants of emerging concern [7]. Improper treatment and management of reclaimed wastewater can pose a risk to human health through the ingestion of food irrigated with reclaimed water. In this respect, regulatory legislation is becoming more and more demanding. The new European regulation (2020/741) for water reuse in agriculture includes the control of a greater number of biological agents than current Spanish legislation (RD 1620/2007), as well as the control of certain contaminants of emerging concern, with the aim of minimising the risks associated with reuse.

Conventional disinfection methods such as chlorination or the use of UV-C radiation are widely used and quite effective in disinfection tasks, but disadvantages such as the formation of highly toxic by-products or the lack of residual effect have motivated research for newer and safer alternatives [8].

Based on the generation of reactive species such as sulfate and hydroxyl radicals, Advanced Oxidation Processes (AOPs) are a promising and versatile alternative to conventional disinfection techniques, as they can remove and even degrade all kinds of pollutants in addition to pathogens [9]. In this scenario, AOPs based on sulfate radicals (SR-AOPs) are gaining popularity, due to their ability to operate in a

* Corresponding authors.
*E-mail addresses:* patricia.gmunoz@upm.es (P. García-Muñoz), jorge.rodriguez.chueca@upm.es (J. Rodríguez-Chueca).

https://doi.org/10.1016/j.jece.2022.108231
Received 13 April 2022; Received in revised form 30 June 2022; Accepted 5 July 2022
Available online 7 July 2022

broader pH range, as well as having a higher oxidation potential and a longer half-life than the commonly employed hydroxyl radical of typical AOPs [10,11].

Among the compounds used for the generation of sulfate radical generation ($SO_4^{\bullet-}$), the peroxymonosulfate (PMS, $HSO_5^-$) is one of the most representative, although it requires previous activation to be effective [12]. This activation can take place, for instance, under exposure to an energy source where the O-O bond suffers from breaking, releasing the reactive species. Specifically, when using UV radiation, the process is known as photolytic activation [10,13], and the reaction that takes place is as described in the Eq. (1).

$$HSO_5^- \xrightarrow{h\nu} SO_4^{\bullet-} + HO^{\bullet} \quad (1)$$

PMS can also be activated by electron transfer as part of homogenous or heterogeneous systems. The first uses transition metals in solution, such as iron, since its reduction potential promotes the dissociation of the oxidant (see Eq. 2),

$$HSO_5^- + Fe^{2+} \rightarrow Fe^{3+} + SO_4^{2-} + HO^{\bullet} \quad (2)$$

While heterogeneous systems are mainly based on the use of a semiconductor, also known as a photocatalyst. When exposed to a source of radiation, these materials generate an electron-hole pair that triggers multiple redox reactions [14,15].

Recently, several works have reported the use of PMS activated by iron-based homogeneous and heterogeneous (photo)catalytic systems [18–21]. For example, gallic acid was used to help reduce dissolved iron (III) to iron (II) and inhibit its reoxidation making it available until the addition of PMS into the system [16]. But the disadvantages of any homogeneous system are obvious, the difficulty of the catalyst recovery and so its reuse make it a nonviable treatment. For heterogeneous systems, it should be said that transition metals play a critical role due to their capacity to act as an electron donor to activate PMS [15]. Several works with iron-containing catalysts have recently been used for sulfate radicals generation [17,18]. For example, a double hydroxide nanosheet catalyst has been developed for the application on the removal of fluoroquinolones in water and a core-shell $Fe_0$ @$Fe_3O_4$ photocatalyst for another antibiotic depletion, sulfamethoxazole [19]. On the other hand, Rodríguez-Chueca et al. reported the use of magnetic $CoFe_2O_4$ to activate PMS and successfully reduce the population of *Enterococcus sp.* and *E.coli* in wastewater samples [20–22]. However, the cost associated with the synthesis and production of those materials causes a decrease in their overall viability.

In this sense, the employment of a natural material could diminish the cost of the overall process since reagent precursors are not needed.

Originally used to obtain $TiO_2$, ilmenite ($FeTiO_3$) is a very promising photocatalyst due to its low cost and high content in iron and titanium [24], which confers excellent (photo)catalytic properties. No previous work on the PMS/Ilmenite/UV-A system for disinfection purposes was found, so using the available literature on all individual elements, the following mechanism is proposed (see Eqs. (3)–(12)) taking into account not only photocatalytic activity, but also catalytic properties due to the presence of iron on the ilmenite surface [10,24,25]:

$$HSO_5^- + ILM - Fe(II) \rightarrow ILM - Fe(III) + SO_4^{\bullet-} + HO^{\bullet} \quad (3)$$

$$HSO_5^- + ILM - Fe(III) - OH \rightarrow ILM - Fe(II) + SO_5^{\bullet-} + H_2O \quad (4)$$

$$ILM - TiO_2 - FeTiO_3 \xrightarrow{h\nu} e_{bc}^- + h_{bv}^+ \quad (5)$$

$$\left(e_{bc}^-\right) + O_2 \rightarrow O_2^{\bullet-} \quad (6)$$

$$\left(h_{bv}^+\right) + H_2O \rightarrow HO^{\bullet} + H^+ \quad (7)$$

$$HSO_5^- + H^{\bullet} \rightarrow SO_4^{\bullet-} + H_2O \quad (8)$$

$$SO_4^{\bullet-} + H_2O \rightarrow H^+ + SO_4^{2-} + HO^{\bullet} \quad (9)$$

$$SO_4^{\bullet-} + ILM - Fe(II) + HO - \rightarrow SO_4^{2-} + ILM - Fe(III) - OH \quad (10)$$

$$ILM - Fe(II) + \left(h_{bv}^+\right) \rightarrow \quad ILM - Fe(III) \quad (11)$$

$$ILM - Fe(III) + \left(e_{bc}^-\right) \rightarrow \quad ILM - Fe(II) \quad (12)$$

On the basis of the previous literature, this work aims to assess the use of a natural mineral, ilmenite, as a catalyst for the activation of PMS under UV-A radiation for the inactivation of *Enterococcus sp.* in simulated wastewater samples, which, to the best of our knowledge, has not been done until now.

*Entereococcus sp.* was chosen as model bacteria for several reasons including that i) it represents an indicator of faecal pollution but also, ii) an indicator of water quality and besides that, iii) it is more resistant to be eliminated than other bacteria, like for instance, *Escherichia coli.*

For this purpose, a series of tests were performed to determine the optimum experimental parameters evaluating initial catalyst and PMS dose, the initial pH as well as the flow rate of the system. Furthermore, the main species involved in the disinfection process were evaluated via quenching experiments, as well as the effect of increased water complexity on the activity of the PMS/Ilmenite/UV-A combined process.

## 2. Materials and methods

### 2.1. Synthetic wastewater samples

The tests were carried out on samples emulating the effluent after secondary wastewater treatment. This water matrix was used to keep the same physicochemical and biological characteristics as the real treated wastewater while maintaining the reproducibility of the experiments. The composition of this simulated wastewater is composed of the following components: urea (Scharlau; 6 mg/L), meat peptone (Scharlau; 32 mg/L), meat extract (Scharlau; 22 mg/L), sodium chloride (Scharlau; 7 mg/L), calcium chloride (Scharlau; 4 mg/L), potassium dihydrogen phosphate (Scharlau; 28 mg/L) and magnesium sulfate (Scharlau; 2 mg/L) [26].

### 2.2. Chemical reagents

In addition to the chemicals listed in the previous section, the following were required to carry out the different experiments: as main reagents, peroxymonosulfate (PMS; $HSO_5^-$; Sigma-Aldrich) in 0.1 mM dosage and ilmenite ($FeTiO_3$; Marphil S. L. Ref.50,110,700), doses ranging from 0.01 to 5 g/L.

The raw ilmenite used as catalyst was previously characterized by García-Muñoz et al. (2016) [23] and showed a 15/85 rutile to ilmenite ratio, a content of 36% in iron, 37% in titanium and a Fe(II) to Fe(III) ratio of 0.56. Before use, ilmenite was milled to a diameter of less than 100 μm.

Additionally, sodium hydroxide (NaOH; Panreac) was used for pH adjustments and methanol (MeOH; $CH_4O$; Panreac), tert-butyl alcohol (TBA; $C_4H_{10}O$; Scharlau), furfuryl alcohol (FFA; $C_5H_6O_3$; Aldrich) and copper nitrate trihydrate ($Cu(NO_3)_2.3\ H_2O$; Panreac) as radical scavengers in a 10: 1 ratio scavenger to oxidant. Sodium persulfate ($Na_2S_2O_8$; Scharlau), sodium sulfite ($Na_2SO_3$; Chem-Lab) and hydrogen peroxide 30% w/w ($H_2O_2$; Scharlau) were used as alternative oxidants instead of PMS. Lastly, calcium carbonate ($CaCO_3$; Scharlau) was added to mimic the hardness of the water during some of the tests, along with sodium nitrate ($NaNO_3$; Scharlau) and trisodium phosphate ($Na_3PO_4$; Scharlau) simulating the presence of nutrients.

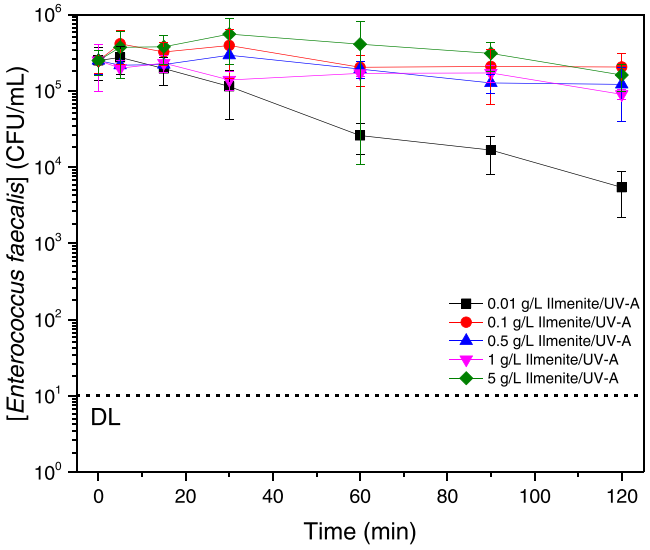


**Fig. 1.** *Enterococcus faecalis* removal by the photocatalytic effect of ilmenite under UV-A. Catalyst doses ranging from 0.01 to 5 g/L of ilmenite.

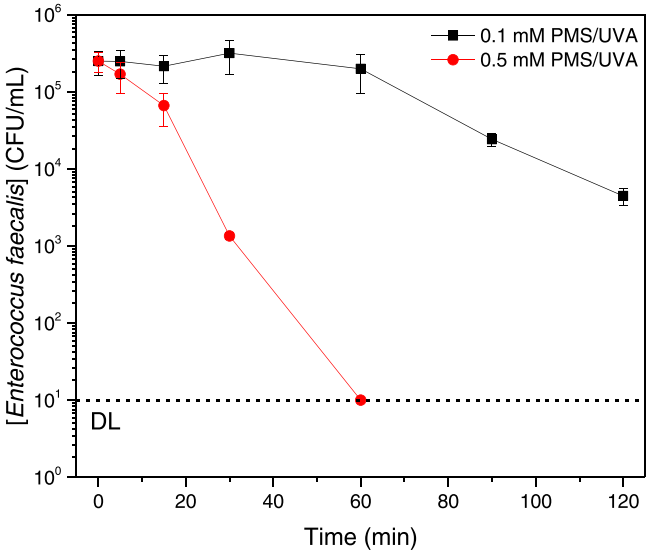


**Fig. 2.** *Enterococcus faecalis* removal by using the PMS/UV-A system with different doses of PMS.

### 2.3. Microbiological analysis

Simulated wastewater samples were doped with a commercial strain of *Enterococcus faecalis* (ATCC 29212, Scharlab). A fresh liquid culture of *Enterococcus faecalis* was prepared in Luria-Bertani nutrient medium (LB broth, Scharlau) after 20 h of incubation at 37 °C. The bacterial suspensions were harvested by centrifugation at 4500 r.p.m. for 15 min. The bacterial pellet was re-suspended in a sterile saline solution (NaCl 0.9%) and diluted in the reactor at an initial concentration of $10^6$ CFU/mL. The collected samples were cultured and enumerated through a serial 10-fold dilution in sterile saline solution (NaCl 0.9%) using the drop plate method and the spread plate method. The diluted samples were plated on Slanetz&Bartley agar (Scharlau; Spain). Colonies were counted after incubation at 37 °C and 48 h. The detection limit (DL) of this experimental procedure was in the range of 10 and 100 CFU/mL depending on the amount of water sample plated.

### 2.4. Experimental setup

The experimental setup consisted of an annular lab scale reactor of 0.252 L with a UV-A lamp (Phillips TL 6 W BLB, $\lambda = 360$ nm) adjusted to work at an irradiance of 14 W $m^{-2}$ inserted in its axis. The tests were carried out in batch recirculation mode using a magnetically coupled pump (Flojet; 230 V, 50 Hz; Input 84 W; Output 18 W). The flow rate was adjusted in the range of 0.2–2 L/min, and after 10 min of circulating through the system to ensure homogeneity of the sample, the pertinent reagents were added, also turning on the UV-A lamp as well.

Blanks experiments were performed also in order to control the activity of the system. This data is available in the previous work of Guerra-Rodríguez et al. [27]. Using only UVA for the inactivation of *Enterococcus sp.* there was no decrease in the inactivation rate for 2 h of photoreaction, while using the PMS the decrease reached half of one order of magnitude with respect to the initial concentration in 2 h of reaction.

## 3. Results and discussion

### 3.1. Photoactivation of Ilmenite

Ilmenite was tested individually as a photocatalyst to determine its efficacy for the inactivation of *Enterococcus faecalis* when exposed to UV-A radiation (365 nm, 14 $Wm^{-2}$). Experiments carried out with catalyst doses ranging from 0.01 to 5 g/L showed that lower catalyst concentrations yielded the best catalytic results in terms of *Enterococcus faecalis* reduction, since an excess of ilmenite in the system had demonstrated turbidity issues and did not allow proper radiation exposure (Fig. 1). Therefore, using an ilmenite dose of 0.01 g/L reached a reduction in the bacteria population of 1.7 log, while the use of higher doses does not achieve reduction results higher than 0.5 log. These results are consistent with those of previous works by García-Muñoz et al. [23,28,29] using ilmenite for the photodegradation of organic pollutants under similar experimental conditions where, achieving a determined catalyst concentration, the system sharply reduced its activity. However, this contrasts with the results presented by Xia et al. [30], where an increase in *Escherichia coli* population killing performance was observed as ilmenite concentration increases.

Although the operating conditions of Xia et al. (UV–vis radiation; *Escherichia coli* as the target pathogen; reactor configuration; etc.) are different from those applied in the present study (UV-A radiation; *Enterococcus faecalis* as the target pathogen; batch reactor with recirculation), the differences in the results of both studies are considerable [30] and may be explained in some extent by different photoreactor configurations, characterized by higher irradiated surface/volume ratios in the work of Xia and co-workers [30]. Nonetheless, both studies show that an increase in the concentration of ilmenite is counterproductive because it leads to higher turbidity and, therefore, to a lower degree of radiation introduction. In addition, the use of an irradiation source centered on the UVA spectrum in this work, makes all photons potentially usable for ilmenite activation (band gap ~2.4 eV). Thus, ilmenite concentration required to observe significant reductions in bacterial population is reduced by up to 50 times compared to that required in the presence of visible radiation.

It should be noted that the rutile present in the structure of the catalyst could be largely responsible for its photocatalytic activity since it acts as a semiconductor when exposed to a source of radiation, as described in Eqs. (14)–(19). However, this mechanism could be inhibited by the presence of Fe(II) and Fe(III) inside the mineral structure, which can accept the photogenerated electron/hole charges that inhibit the photocatalytic process by oxidizing/reducing to Fe(II) or Fe (III), respectively, and thus reducing the oxidizing activity [23].

$$TiO_2 \xrightarrow{h\nu} TiO_2(e^-_{bc} + h^+_{bv}) \quad (14)$$

$$TiO_2(h^+_{bv}) + H_2O_{ad} \rightarrow TiO_2 + HO^{\bullet} + H^+ \quad (15)$$

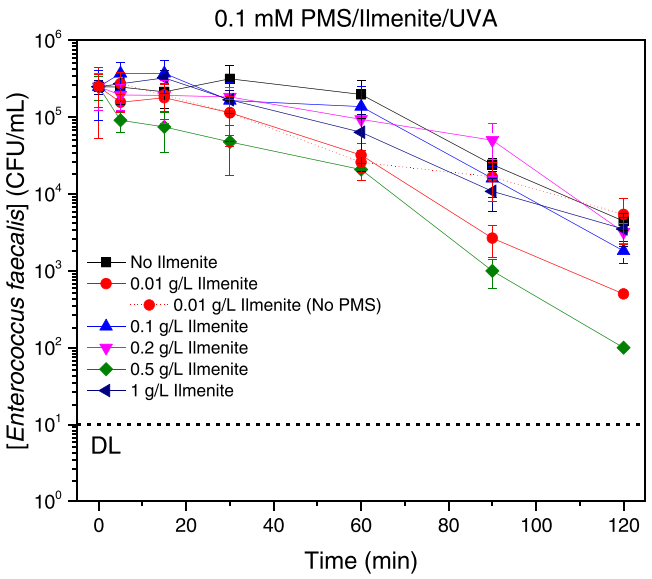


**Fig. 3.** Ilmenite optimization loading for *Enterococcus faecalis* inactivation in the presence of UV-A radiation using 0.1 mM of PMS.

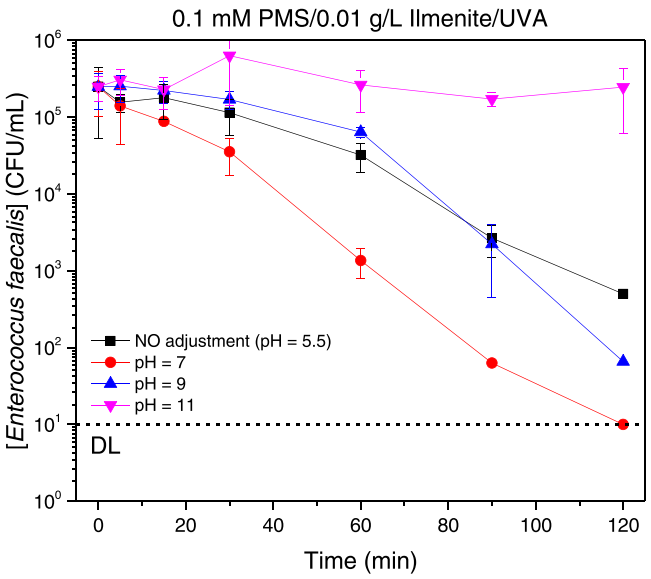


**Fig. 4.** Initial pH effect on *Enterococcus faecalis* inactivation through the PMS/Ilmenite/UV-A system. [Ilmenite] = 0.01 g/L; [PMS] = 0.1 mM.

$$TiO_2\left(h^+_{bv}\right) + OH^-_{ad} \rightarrow TiO_2 + HO^\bullet \quad (16)$$

$$O_2^{\bullet-} + H^+ \rightarrow HO_2^\bullet \quad (17)$$

$$2HO_2^\bullet \rightarrow O_2 + H_2O_2 \quad (18)$$

$$TiO_2\left(e^-_{bc}\right) + H_2O_2 \rightarrow TiO_2 + OH^- + HO^\bullet \quad (19)$$

### 3.2. Photoactivation of PMS

For the purpose of this work, two different doses of PMS (0.1 and 0.5 mM) were tested in the absence of catalyst to remove *Enterococcus faecalis*, according to previous experiences reported by members of the research team [20,31]. Fig. 2 shows the results obtained for disinfection purposes when using the above-mentioned doses of PMS. Unlike ilmenite photoactivity, a direct correlation is observed (Fig. 2) between oxidant dosage and inactivation power, reaching the detection limit halfway through the experiment when working at higher doses, which means a faster disinfection rate was obtained. However, some authors have reported that a higher dose of PMS can scavenge the free radicals generated as a consequence of secondary reactions [13].

Previous studies have shown variable results when testing PMS against different microbiological species. Rodríguez-Chueca et al. (2019) [31] observed that when trying to inactivate *Escherichia coli* and *Enterococcus sp.* simultaneously, the detection limit was reached much quicker in the first, showing that while the PMS/UV-A system is effective and versatile, the resilience of pathogens plays a crucial role in setting the optimal operation parameters confirming the authors stated before. On the other hand, the disinfection of water matrices with the PMS/UV system has been widely reported [9,32,33] and it is well-known the mechanisms and optimal conditions to reach total inactivation of pathogens. Therefore, the results shown in Fig. 2 are intended only as a baseline comparison of the individual effects of each of the reagents that will make up the PMS/Ilmenite/UV-A system. Finally, although a PMS concentration of 0.5 mM allows a rapid elimination of *Enterococcus faecalis* to be obtained, its use in further experiments in combination with ilmenite is ruled out to adequately follow the kinetics of elimination of this pathogenic bacterium.

### 3.3. PMS/Ilmenite/UV-A system optimization

After carefully analyzing the influence of each parameter individually, the catalytic ability of the PMS/Ilmenite/UVA system for the inactivation of *Enterococcus faecalis*. In Fig. 3 can be seen the more relevant results obtained for a catalyst dose ranging from 0.01 to 1 g/L since concentrations over 1 g/L and using a dose of PMS of 0.1 mM seemed not to improve the activity. It should be noted that, as previously reported [23,34], the optimum photocatalyst dose and the optimum catalyst concentration for the combined process are not similar.

Fig. 3 shows the positive effect that the addition of a moderate dose of ilmenite (0.5 g/L) has on the combined PMS/UV-A system, while doubling the dose (1 g/L), the improvement is hardly noticeable. Despite the screen effect already mentioned in the pure photocatalytic results (Fig. 1), the disinfection activity increased when working at higher doses of ilmenite. This can be explained because PMS activation is associated not only by the light effect, but also with the catalytic activity of the ilmenite surface [23]. The presence of iron has been reported to activate certain sulfate species, leading to radical formation and provoking the subsequent disinfection reaction [31].

All the tests carried out to find the optimum dose of ilmenite appear to follow a consistent inactivation pattern, as shown in Fig. 3: the pathogen population hardly decreases during the first half of the experiment, then enters more of an active phase in which most of the disinfection process takes place. This phenomenon could be ascribed to the Fe(III) present on the catalyst surface. Constantly reducing to Fe(II) when exposed to radiation (Eq. 20), it triggers the reaction rate after reaching a certain concentration on the surface of the mineral [23,35].

$$\text{ILM} - Fe(III) \xrightarrow{h\nu} ILM - Fe(II) \quad (20)$$

Although according to Fig. 3 the highest disinfection performance of *Enterococcus faecalis* occurs with the combination of 0.1 mM PMS, 0.5 g/L of ilmenite in the presence of UV-A radiation, it was decided to take as working conditions the 0.01 g/L dose of ilmenite, as it obtained similar results in terms of disinfection, with a concentration 50 times lower.

#### 3.3.1. pH and flowrate influence

This set of reactions is devoted to determining whether, at optimum pH, a complete inactivation could be achieved when working at a catalyst load of 0.01 g/L and 0.1 mM PMS dose as a typical PMS concentration employed for these processes. Assuming that the raw sample

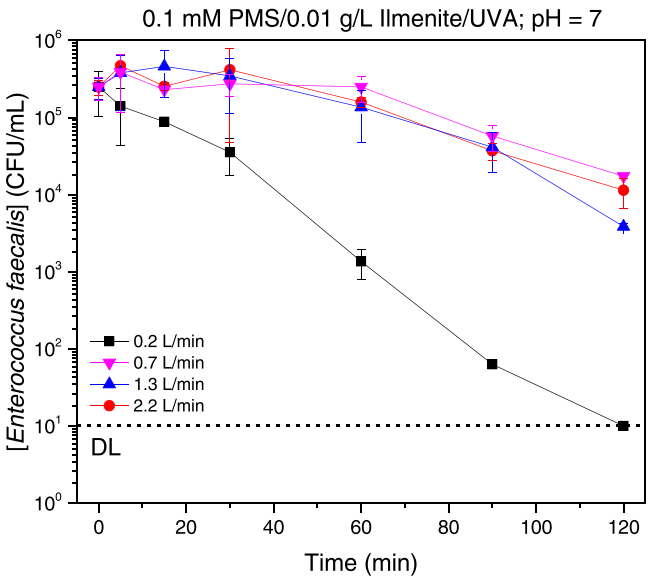


**Fig. 5.** Flowrate effect on the activity of the combined system. Working conditions: [Ilmenite] = 0.01 g/L; [PMS] = 0,1 mM; UV-A; $pH_0$ = 7.

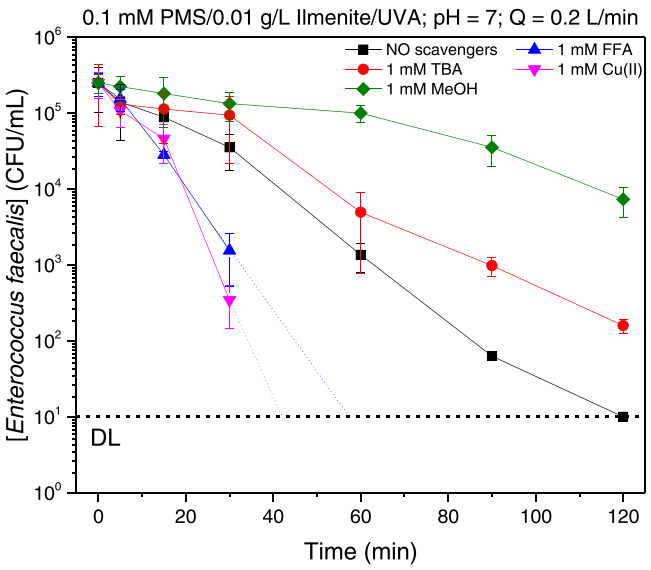


**Fig. 6.** Test performed in the presence of different scavengers in the optimized system. Conditions: [Ilmenite] = 0.01 g/L; [PMS] = 0.1 mM; UV-A; $pH_0$ = 7.

has a natural pH value of 5.5, tests at varied initial pH values of 7, 9 and 11 were carried out too. Therefore, Fig. 4 plots the inactivation values of *Enterococcus faecalis* using the optimal conditions previously reached in the previous section, using different pH values. In Fig. 4 it can be inferred that in our case, the optimum working initial pH is centered on neutral values (≈ 7) and that lower and higher initial values provoke a reduction in the disinfection process. Furthermore, it must be noted that total bacteria depletion was reached in 120 min when working at $pH_0$ = 7.

Previous work testing similar systems clearly showed how initial pH is heavily linked to the reactive species present during the disinfection process due to the $SO_4^{\bullet-}$ decomposition once is formed. However, the study concludes that both $HO^{\bullet}$ and $SO_4^{\bullet-}$ species dominate the process of PMS activation [21]. Despite this, Wang and Wang [13] also reported that *once* $SO_4^{\bullet-}$ is formed, it can follow three ways: i) it remains the predominant specie at pH < 7, ii) it decomposes to $HO^{\bullet}$ y $SO_4^{\bullet-}$ at pH = 9, and iii) it its transformed to $HO^{\bullet}$ and $SO_4^{2-}$ at pH around 12, confirming that the highest organic pollutant removal yields are obtained when operating in a pH range between 7 and 8 due to the existence of more oxidizing radicals. It is also important to note the decomposition of PMS through alkaline activation of PMS, where superoxide radical and singlet oxygen have been shown to be the predominant species [13]. However, and based on what is observed in Fig. 4, this activation pathway has a clearly lower performance than that obtained by the photocatalytic treatment system at neutral pH.

The lack of information available on the PMS/ILM/UV-A system does not allow us to compare thoroughly with other catalytic results. Similar works lead to the notion that the optimal initial pH depends on the nature of the (photo)catalyst, the oxidant and the targeted pollutants, as well as their concentrations in water [23,25,36].

Finally, the influence of flow rate on disinfection rates was also studied. Different flow rates were tested, showing that longer retention and illumination times yield significantly better results. Therefore, Fig. 5 plots the inactivation of *Enterococcus faecalis* with optimal operating conditions and using different flow rates ranging between 0.2 and 2.2 L/min. This suggests that there is a minimum radiation exposure period required to trigger the disinfection process, as depicted in Fig. 5. The optimal flow rate was obtained for 0.2 L / min, a value considered as fixed for the next experiments.

### 3.4. Scavenger tests

A series of experiments involving scavengers were performed to gain insight into the reaction mechanisms of the PMS/Ilmenite/UV-A system and to try to show a plausible mechanism for bacteria inactivation. To do this, a set of scavengers capable of selectively trapping possible free and oxidative species formed in the PMS/ilmenite/UVA system was used. None of the reagents used for this purpose showed any disinfectant action when tested individually. The disinfectant action was previously tested by adding a 10 mM scavenger dosage to a pathogen load of approximately $10^6$ CFU/mL of *Enterococcus faecalis* suspended in 0.9% saline (data not shown).

Fig. 6 shows the results of the quenching tests using a final scavenger concentration of 1 mM. MeOH and TBA worked as expected: the first one trapped $HO^{\bullet}$ and $SO_4^{\bullet-}$ radicals, overriding the disinfection process almost completely (1.5-log reduction), while the latter reacted exclusively to sulfate radicals and therefore had much less of an impact on the final performance (3.2-log reduction). The outcome of these two experiments indicates that both radicals could be responsible for the inactivation of *Enterococcus faecalis* in this system, being the most prevalent the $HO^{\bullet}$. This is in good agreement with the work of Zeng et al. (2021) [37], where at neutral pH one of the main radicals responsible for the disinfection process was $HO^{\bullet}$.

FFA was used with the objective of identifying $^1O_2$ formation in the PMS/Ilmenite/UVA reaction as reported by other authors in similar treatments [38–40]. However, tests involving FFA could not confirm the presence of $^1O_2$ in the process. Contrary to what was expected, as shown in Fig. 6, the kinetic in *Enterococcus faecalis* inactivation increased in the presence of FFA, reaching the detection limit in only 60 min, in other words, half as much time as in the absence of FFA. The reason why this occurs is not easily identifiable by the authors and should require further study using quantitative free radical detection technologies such as EPR. However, given the lack of access to these techniques, the authors attempt to hypothesize on the basis of experiences described in the literature. Richard and Lemaire [41] studied the phototransformation of furfuryl alcohol in aqueous ZnO suspensions. The study of intermediate species by Richard and Lemaire [41] reported the occurrence of two species, 6-hydroxy-2 H) -pyran-3- (6 H) -one and furan-2-carbocaldehyde. The study of the mechanism to arrive at the latter intermediate determined that a hydroperoxyl radical ($HO_2^{\bullet}$) was released, which, as is well known, has an oxidizing capacity. Therefore, this species could contribute to the speed of inactivation of *Enterococcus*

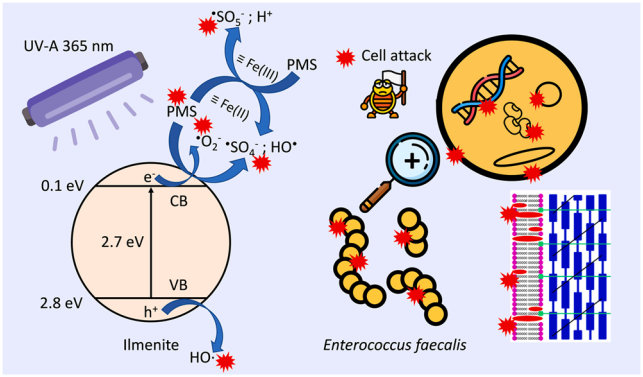


**Fig. 7.** Plausible mechanism of photocatalytic inactivation of *Enterococcus faecalis* in the PMS/Ilmenite/UVA process.

*faecalis*. However, this is not the only possibility for the appearance of oxidizing species through the use of FFA. Deo et al. [42] reported the reaction paths for the hydrodeoxygenation of FFA at $TiO_2$/Pd interfaces. During the hydrodeoxygenation of FFA, the production of hydroxyl radicals (HO •) has been reported [42], therefore, the increase in the production of one of the main free species with oxidative capacity could be one of the reasons for the increased inactivation kinetics of *Enterococcus faecalis*. Furthermore, Wang et al. [43] have recently advised against the use of alcohols as scavengers for the determination of hydroxyl radicals, because in combination with UV radiation significant amounts of hydrogen peroxide are detected, which in turn is a precursor for the formation of new hydroxyl radicals. This fact could be another hypothesis that could explain the increase in the kinetics of bacterial inactivation. Furthermore, all these hypotheses could be completed by the fact that the FFA itself is rapidly disappearing from the reaction as a consequence of a decomposition reaction as a consequence of the system under study (PMS/Ilmenite/UVA). Several authors have used FFA itself as a target pollutant to test the efficacy of different oxidation treatments [44,45]. Its rapid removal is therefore a problem for its own performance as a scavenger, and, on the other hand, the removal may actually be a transformation to intermediate species such as those discussed above. In this regard, the authors suggest that perhaps the presence of FFA could reduce the recombination of charges, provoking a higher production of $HO_2$·and HO·and leading to a higher disinfection rate.

Finally, it was decided to use Cu(II) as an electron scavenger, as reported by numerous authors [46]. However, Cu(II) behaved in the same way as FFA, increasing the kinetic of inactivation of *Enterococcus faecalis*. However, the reason for the increased reaction kinetics is much clearer. Firstly, Cu has antibacterial properties, so its presence can lead to inactivation of the bacteria under study [47]. Second, Cu (II) has been successfully tested as an activator of PMS and PDS, so its presence in water, instead of trapping electrons, causes an increase in the kinetics of PMS decomposition, increasing the rate of generation of free species [24, 48]. Third, when Cu (II) captures electrons, again, the recombination rate of the photocharges is substantially reduced, provoking a faster disinfection rate.

Fig. 7 attempts to schematize the plausible mechanism of the formation of these oxidizing species, and the main points of attack on *Enterococcus faecalis*. Disinfection processes are quite complex to understand, and there are multiple causes of cell inactivation and/or death. One of the main damages caused by oxidizing species is to the cell membrane of microorganisms. In the case of Gram-positive bacteria such as *Enterococcus faecalis*, this membrane is thicker than those of Gram-negative bacteria and, although in principle it may be more resistant to oxidative treatments, it eventually causes irreparable damage to the cell. Fracture of the cell membrane causes oxidative agents to enter the cell interior, causing significant damage to both enzymes, such as catalase (CAT) and superoxide dismutase (SOD), and DNA [49,50].

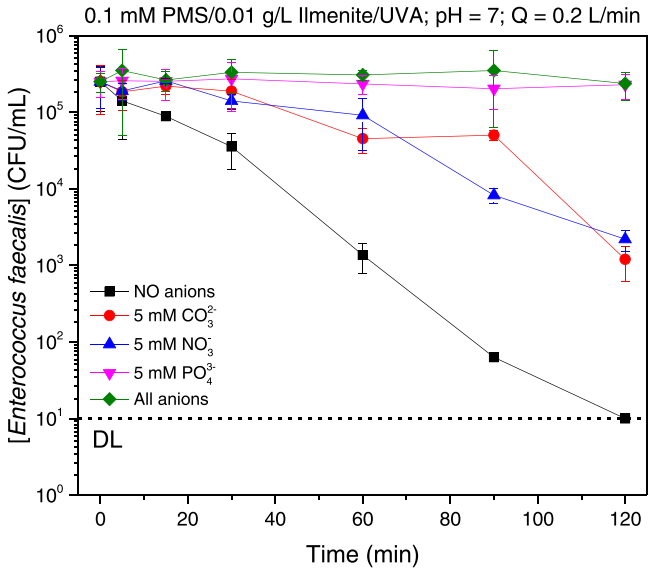


**Fig. 8.** Effect of the complexity of the matrix on the disinfection process. Conditions: [Ilmenite] = 0.1 g/L, [PMS] = 0.01 mM; $pH_0$ = 7, UV-A.

### 3.5. The influence of the water matrix

To know the performance of the system when the complexity of the water matrix increased, reactions with several ionic species were carried out, which allowed one to understand the limits of the treatment depending on the presence of inorganic substances that are typical in natural and waste waters. The presence of certain compounds, such as organic matter or carbonates, which are easily found in municipal wastewater, has been extensively studied [51], but it is required for other substances.

Fig. 8 shows how water hardness ($CO_3^{2-}$) and the presence of nutrients ($NO_3^-$ and $HPO_4^{2-}$) in the aqueous matrix hindered the performance of the PMS/Ilmenite/UV-A system in all cases. According to Fig. 8, the addition of $CO_3^{2-}$, $NO_3^-$ and $HPO_4^{2-}$ considerably reduced the *Enterococcus faecalis* inactivation through the optimized process. It should be noted that the inactivation efficiency of the treatment disappears completely when hydrogen phosphate is added, and of course also when all the anions studied are present in the water. When carbonates and nitrates are added to the water, the decrease in treatment effectiveness is halved compared to optimized treatment on simulated wastewater, reaching removal efficiencies between 2 and 2.5 log in 120 min

Kiejza et al. [24] reported that these three anions act as radical scavengers. For instance, carbonate ($CO_3^{2-}$) and bicarbonate ($HCO_3^{2-}$) anions work as sulfate and hydroxyl radical scavengers forming less reactive species as follows as described in Eqs. (21)–(24) [24]:

$$CO_3^{2-} + H_2O \rightarrow OH^- + HCO_3^- \quad (21)$$

$$SO_4^{\bullet-} + HCO_3^- \rightarrow HCO_3^{\bullet} + SO_4^{2-} \quad (22)$$

$$SO_4^{\bullet-} + CO_3^{2-} \rightarrow CO_3^{\bullet-} + SO_4^{2-} \quad (23)$$

$$HO^{\bullet} + CO_3^{2-} \rightarrow CO_3^{\bullet-} + OH^- \quad (24)$$

In the same way, nitrate anions ($NO_3^-$), when present in high concentrations, trap sulfate radicals according to Eqs. (25) and (26) [24]:

$$NO_3^- + H_2O \xrightarrow{h\nu} NO_2^{\bullet} + HO^{\bullet} + OH^- \quad (25)$$

$$SO_4^{\bullet-} + NO_3^- \rightarrow NO_3^{\bullet} + SO_4^{2-} \quad (26)$$

In the case of nitrates, as shown in Eqs. (25) and (26), the reaction leads to the appearance of nitrite and nitrate radicals, but the oxidation

**Table 1**
Latest work reported in literature including the E. feacelis inactivation by photoassisted AOP processes.

| Process | Pathogen / Pollutant | Conditions | Yield | Reference |
|---|---|---|---|---|
| Photocatalytic ZnO and B-ZnO | *E.coli* and *Enterococcus* sp. | $10^6$ initial CFU $mL^{-1}$ from each bacteria | ZnO and B-ZnO materials reached 6-log during 30 min and 60 min of lighting, respectively. | Nuñez-Salas et. al.[21] |
| Solar photo-Fenton with EDDS complex | *E. coli* and *E. faecalis* | $10^6$ initial CFU $mL^{-1}$ from each bacteria | *E. coli* (6 log reduction) with 14.5 kJ/L of $Q_{UV}$. The concentration of *E. faecalis* only decreased 4 log for the same $Q_{UV}$. | García-Fernández et al. [53] |
| Sulfate radicals | *E. faecalis* and degradation of carbamazepine | *Initial E. faecalis* concentration $7.37{\cdot}10^{-6}$ M. | *K* of *E. faecalis* reacting with $SO_4^{\bullet-}$ was determined to be $5.42{\cdot}10^9$ $M^{-1}{\cdot}s^{-1}$. | Liu et al.[54] |
| Solar photo-activated persulfate | *E. coli* and *E. faecalis* | $10^6$ initial CFU $mL^{-1}$ from each bacterium | 6-Log Reduction Value in *E. coli* and *E. faecalis* was observed after solar exposure periods of 20 min, using 0.5 and 0.7 mM of PS, respectively. | Ferreira et al. [55] |
| Persulfate processes | *E. coli and E. faecalis* | $10^6$ initial CFU $mL^{-1}$ from each bacterium | 6-log reduction in 30 min (persulfate and dissolved iron) | Venieri et al.[56] |
| $CoFe_2O_4$ ferrite for PMS activation | *E. coli* and *Enterococcus sp.* | $10^6$ initial CFU $mL^{-1}$ from each bacterium | 6-log reduction in 30 and 60 min for *E.coli* and *Enterococcus sp.*, respectively | Rodríguez-Chueca[57] |
| ZVI/persulfate | *E. faecalis* and carbamazepine | [*E. faecalis*] = $1{\cdot}10^7$ CFU $mL^{-1}$, [CBZ] = 10 μM | 73.8% of inactivation in 12 min, 42.3% reduction of the initial concentration of CBZ | Liu et al.[58] |
| UVC+persulfate | *E. coli and E. faecalis* and Emerging Pollutants | initial concentration of $10^6$ CFU/mL of each bacterium | *E. coli* > *E. faecalis* and DCF > TMP ≅ SMX. | Berruti et al.[59] |
| α-$Fe_2O_3$ /oxone | *E. coli* and *E. faecalis* and Emerging Pollutants | $10^6$ CFU/mL initial bacteria concentration | *Disinfection in 15 min of reaction* | Mohammadi et al.[60] |
| ZVI/persulfate system | *Escherichia coli* and *Enterococcus faecalis* in municipal wastewater | The initial of *E. coli* and *E. faecalis* for disinfection experiments were set to about $1.07{\cdot}10^7$ colony—forming unit (CFU) $mL^{-1}$. | *90% of inactivation in 80 min* | Xiao et al.[61] |
| Natural Ilmenite, $FeTiO_3$ | *Enterococcus sp.* | $10^6$ initial CFU $mL^{-1}$ | 6-log reduction in 120 min | This work |

potentials of these species are lower than those of the trapped sulfate radical. However, this fact may explain why the effectiveness of the treatment is not completely reduced.

Lastly, hydrogenphosphate anions ($HPO_4^{2-}$) quench both sulfate and hydroxyl radicals, overriding totally the process (Eqs. 27 and 28) [24]:

$$HPO_4^{2-} + HO^{\bullet} \rightarrow HPO_4^{-} + OH^{-} \quad (27)$$

$$HPO_4^{2-} + SO_4^{\bullet-} \rightarrow HPO_4^{-} + SO_4^{2-} \quad (28)$$

confirming that the efficiency of the advanced oxidation processes decreases in presence of ions [52].

Due to the scarcity of existing works dealing with the inactivation of *E. feacelis* vs those facing *Escherichia coli*, a summary has been done, for the sake of comparison. In Table 1 can be seen the latest works dealing with the inactivation of bacteria, including E. *faecalis*.

## 4. Conclusions

The PMS/Ilmenite/UV-A system has proven effective for *Enterococcus faecalis* inactivation in synthetic wastewater. While ilmenite and PMS performed poorly when photoactivated individually, the detection limit was reached when paired together at an initial pH of 7 and with optimal doses set at 0.01 g/L and 0.1 mM of ilmenite and PMS, respectively. Quenching tests showed that sulfate and hydroxyl radicals are responsible for both the disinfection process. Furthermore, as expected, when increasing the complexity of the water matrix, it had a negative effect on system efficiency, since calcium carbonate and nutrients act as sulfate and hydroxyl radical scavengers, decreasing *Enterococcus faecalis* inactivation.

## CRediT authorship contribution statement

**Patricia García-Muñoz:** Conceptualization, Methodology, Formal analysis, Investigation, Writing – original draft, Writing – review & editing, Project administration, Funding acquisition, **Jorge Rodríguez-Chueca:** Conceptualization, Methodology, Formal analysis, Investigation, Writing – original draft, Writing – review & editing, Project administration, Funding acquisition, **Cecilia L. Maxías:** Methodology, Investigation, Writing – original draft, **Sonia Guerra-Rodríguez:** Methodology, Investigation, **Jaime Carbajo:** Conceptualization, Writing – review & editing, **José A. Casas:** Conceptualization, Writing – review & editing.

## Declaration of Competing Interest

The authors declare that they have no known competing financial interests or personal relationships that could have appeared to influence the work reported in this paper.

## Data availability

Data will be made available on request.

## Acknowledgement

PGM acknowledges Escuela Técnica Superior de Ingenieros Industriales (UPM) for the project ETSII-UPM20–03. SGR acknowledges UPM for the predoctoral contract granted within the 'Programa Propio'. JRC acknowledges Comunidad de Madrid for funding the research project IN_REUSE (APOYO-JOVENES-X5PKL6–88-KZ46KU), and also by the pluriannual agreement with the Polytechnic University of Madrid in the line of action Programme of Excellence for University Teaching Staff".

## Appendix A. Supporting information

Supplementary data associated with this article can be found in the online version at doi:10.1016/j.jece.2022.108231.

## References

[1] J.C. Semenza, Cascading risks of waterborne diseases from climate change, Nat. Immunol. 21 (2020) 484–487, https://doi.org/10.1038/s41590-020-0631-7.
[2] L. Wang, J. Tong, Y. Li, River chief system (RCS): an experiment on cross-sectoral coordination of watershed governance, Front. Environ. Sci. Eng. 13 (2019), https://doi.org/10.1007/s11783-019-1157-9.
[3] Water safety planning What have we learned so far? THE NEED FOR WATER SAFETY PLANNING, 2019.
[4] P. Kulkarni, N.D. Olson, J.N. Paulson, M. Pop, C. Maddox, E. Claye, R.E. Rosenberg Goldstein, M. Sharma, S.G. Gibbs, E.F. Mongodin, A.R. Sapkota, Conventional wastewater treatment and reuse site practices modify bacterial community structure but do not eliminate some opportunistic pathogens in reclaimed water,

Sci. Total Environ. 639 (2018) 1126–1137, https://doi.org/10.1016/j.scitotenv.2018.05.178.
[5] R. Mosteo, M.P. Ormad, P. Goñi, J. Rodríguez-Chueca, A. García, A. Clavel, Identification of pathogen bacteria and protozoa in treated urban wastewaters discharged in the Ebro River (Spain): water reuse possibilities, Water Sci. Technol. 68 (2013) 575–583, https://doi.org/10.2166/wst.2013.201.
[6] A. López, J. Rodríguez-Chueca, R. Mosteo, J. Gómez, E. Rubio, P. Goñi, M. P. Ormad, How does urban wastewater treatment affect the microbial quality of treated wastewater? Process Saf. Environ. Prot. 130 (2019) 22–30, https://doi.org/10.1016/j.psep.2019.07.016.
[7] R. Delli Compagni, M. Gabrielli, F. Polesel, A. Turolla, S. Trapp, L. Vezzaro, M. Antonelli, Risk assessment of contaminants of emerging concern in the context of wastewater reuse for irrigation: an integrated modelling approach, Chemosphere 242 (2020), https://doi.org/10.1016/j.chemosphere.2019.125185.
[8] S.W. Krasner, H.S. Weinberg, S.D. Richardson, S.J. Pastor, R. Chinn, M.J. Sclimenti, G.D. Onstad, A.D. Thruston, Occurrence of a new generation of disinfection byproducts, Environ. Sci. Technol. 40 (2006) 7175–7185, https://doi.org/10.1021/es060353j.
[9] J. Rodríguez-Chueca, C. García-Cañibano, R.J. Lepistö, J. Encinas, J. Pellinen, Marugán, Intensification of UV-C tertiary treatment: disinfection and removal of micropollutants by sulfate radical based Advanced Oxidation Processes, J. Hazard. Mater. (2019) 94–102, https://doi.org/10.1016/j.jhazmat.2018.04.044.
[10] S. Xiao, M. Cheng, H. Zhong, Z. Liu, Y. Liu, X. Yang, Q. Liang, Iron-mediated activation of persulfate and peroxymonosulfate in both homogeneous and heterogeneous ways: A review, Chem. Eng. J. 384 (2020), https://doi.org/10.1016/j.cej.2019.123265.
[11] Y. Tao, Q. Ni, M. Wei, D. Xia, X. Li, A. Xu, Metal-free activation of peroxymonosulfate by g-C3N4 under visible light irradiation for the degradation of organic dyes, RSC Adv. 5 (2015) 44128–44136, https://doi.org/10.1039/c5ra06223c.
[12] S. Guerra-Rodríguez, E. Rodríguez, D.N. Singh, J. Rodríguez-Chueca, Assessment of sulfate radical-based advanced oxidation processes for water and wastewater treatment: A review, Water (Switz. ) 10 (2018), https://doi.org/10.3390/w10121828.
[13] J. Wang, S. Wang, Activation of persulfate (PS) and peroxymonosulfate (PMS) and application for the degradation of emerging contaminants, Chem. Eng. J. 334 (2018) 1502–1517, https://doi.org/10.1016/j.cej.2017.11.059.
[14] X. Zhou, Q. Zhao, J. Wang, Z. Chen, Z. Chen, Nonradical oxidation processes in PMS-based heterogeneous catalytic system: generation, identification, oxidation characteristics, challenges response and application prospects, Chem. Eng. J. 410 (2021), https://doi.org/10.1016/j.cej.2020.128312.
[15] M. Kohantorabi, G. Moussavi, S. Giannakis, A review of the innovations in metal- and carbon-based catalysts explored for heterogeneous peroxymonosulfate (PMS) activation, with focus on radical vs. non-radical degradation pathways of organic contaminants, Chem. Eng. J. 411 (2021), https://doi.org/10.1016/j.cej.2020.127957.
[16] T. Pan, Y. Wang, X. Yang, X. fei Huang, R. liang Qiu, Gallic acid accelerated BDE47 degradation in PMS/Fe(III) system: oxidation intermediates autocatalyzed redox cycling of iron, Chem. Eng. J. 384 (2020), https://doi.org/10.1016/j.cej.2019.123248.
[17] M. Moazeni, S.M. Hashemian, M. Sillanpää, A. Ebrahimi, K.H. Kim, A heterogeneous peroxymonosulfate catalyst built by Fe-based metal-organic framework for the dye degradation, J. Environ. Manag. 303 (2022), https://doi.org/10.1016/j.jenvman.2021.113897.
[18] G. Zhao, J. Zou, X. Chen, L. Liu, Y. Wang, S. Zhou, X. Long, J. Yu, F. Jiao, Iron-based catalysts for persulfate-based advanced oxidation process: microstructure, property and tailoring, Chem. Eng. J. 421 (2021), https://doi.org/10.1016/j.cej.2020.127845.
[19] S. Wang, J. Wang, Synergistic effect of PMS activation by Fe0@Fe3O4 anchored on N, S, O co-doped carbon composite for degradation of sulfamethoxazole, Chem. Eng. J. 427 (2022), https://doi.org/10.1016/j.cej.2021.131960.
[20] J. Rodríguez-Chueca, E. Barahona-García, V. Blanco-Gutiérrez, L. Isidoro-García, A.J. dos santos-García, Magnetic CoFe2O4 ferrite for peroxymonosulfate activation for disinfection of wastewater, Chem. Eng. J. 398 (2020), https://doi.org/10.1016/j.cej.2020.125606.
[21] R.E. Núñez-Salas, J. Rodríguez-Chueca, A. Hernández-Ramírez, E. Rodríguez, M.D. L. Maya-Treviño, Evaluation of B-ZnO on photocatalytic inactivation of Escherichia coli and Enterococcus sp, J. Environ. Chem. Eng. 9 (2021), https://doi.org/10.1016/j.jece.2020.104940.
[22] S. Iravani, Nanophotocatalysts against viruses and antibiotic-resistant bacteria: recent advances, Crit. Rev. Microbiol. 48 (2022) 67–82, https://doi.org/10.1080/1040841X.2021.1944053.
[23] P. García-Muñoz, G. Pliego, J.A. Zazo, A. Bahamonde, J.A. Casas, Ilmenite (FeTiO3) as low cost catalyst for advanced oxidation processes, J. Environ. Chem. Eng. 4 (2016) 542–548, https://doi.org/10.1016/j.jece.2015.11.037.
[24] D. Kiejza, U. Kotowska, W. Polińska, J. Karpińska, Peracids - New oxidants in advanced oxidation processes: The use of peracetic acid, peroxymonosulfate, and persulfate salts in the removal of organic micropollutants of emerging concern – A review, Sci. Total Environ. 790 (2021), https://doi.org/10.1016/j.scitotenv.2021.148195.
[25] J. Peng, H. Zhou, W. Liu, Z. Ao, H. Ji, Y. Liu, S. Su, G. Yao, B. Lai, Insights into heterogeneous catalytic activation of peroxymonosulfate by natural chalcopyrite: pH-dependent radical generation, degradation pathway and mechanism, Chem. Eng. J. 397 (2020), https://doi.org/10.1016/j.cej.2020.125387.
[26] M.I. Polo-López, I. García-Fernández, T. Velegraki, A. Katsoni, I. Oller, D. Mantzavinos, P. Fernández-Ibáñez, Mild solar photo-Fenton: an effective tool for the removal of Fusarium from simulated municipal effluents, Appl. Catal. B: Environ. 111– 112 (2012) 545–554, https://doi.org/10.1016/j.apcatb.2011.11.006.
[27] S. Guerra-Rodríguez, E. Rodríguez, J. Moreno-Andrés, J. Rodríguez-Chueca, Effect of the water matrix and reactor configuration on Enterococcus sp. inactivation by UV-A activated PMS or H2O2, J. Water Process Eng. 47 (2022), https://doi.org/10.1016/j.jwpe.2022.102740.
[28] P. García-Muñoz, G. Pliego, J.A. Zazo, J.A. Casas, Photocatalytic wet peroxide oxidation process at circumneutral pH using ilmenite as catalyst, J. Environ. Chem. Eng. 6 (2018) 7312–7317, https://doi.org/10.1016/j.jece.2018.10.051.
[29] P. García-Muñoz, G. Pliego, J.A. Zazo, B. Barbero, A. Bahamonde, J.A. Casas, Modified ilmenite as catalyst for CWPO-Photoassisted process under LED light, Chem. Eng. J. 318 (2017) 89–94, https://doi.org/10.1016/j.cej.2016.05.093.
[30] D. Xia, H. He, H. Liu, Y. Wang, Q. Zhang, Y. Li, A. Lu, C. He, P.K. Wong, Persulfate-mediated catalytic and photocatalytic bacterial inactivation by magnetic natural ilmenite, Appl. Catal. B: Environ. 238 (2018) 70–81, https://doi.org/10.1016/j.apcatb.2018.07.003.
[31] J. Rodríguez-Chueca, S. Guerra-Rodríguez, J.M. Raez, M.J. López-Muñoz, E. Rodríguez, Assessment of different iron species as activators of S2O82- and HSO5- for inactivation of wild bacteria strains, Appl. Catal. B: Environ. 248 (2019) 54–61, https://doi.org/10.1016/j.apcatb.2019.02.003.
[32] W. Qi, S. Zhu, A. Shitu, Z. Ye, D. Liu, Low concentration peroxymonosulfate and UVA-LED combination for E. coli inactivation and wastewater disinfection from recirculating aquaculture systems, J. Water Process Eng. 36 (2020), https://doi.org/10.1016/j.jwpe.2020.101362.
[33] Z. Amiri, G. Moussavi, S. Mohammadi, S. Giannakis, Development of a VUV-UVC/peroxymonosulfate, continuous-flow advanced oxidation process for surface water disinfection and natural organic matter elimination: application and mechanistic aspects, J. Hazard. Mater. 408 (2021), https://doi.org/10.1016/j.jhazmat.2020.124634.
[34] P. García-Muñoz, G. Pliego, J.A. Zazo, M. Munoz, Z.M. de Pedro, A. Bahamonde, J. A. Casas, Treatment of hospital wastewater through the CWPO-Photoassisted process catalyzed by ilmenite, J. Environ. Chem. Eng. 5 (2017) 4337–4343, https://doi.org/10.1016/j.jece.2017.08.023.
[35] J.A. Zazo, G. Pliego, P. García-Muñoz, J.A. Casas, J.J. Rodriguez, UV-LED assisted catalytic wet peroxide oxidation with a Fe(II)-Fe(III)/activated carbon catalyst, Appl. Catal. B: Environ. 192 (2016) 350–356, https://doi.org/10.1016/j.apcatb.2016.04.010.
[36] C. Pan, L. Fu, Y. Ding, X. Peng, Q. Mao, Homogeneous catalytic activation of peroxymonosulfate and heterogeneous reductive regeneration of Co2+ by MoS2: The pivotal role of pH, Sci. Total Environ. 712 (2020), https://doi.org/10.1016/j.scitotenv.2019.136447.
[37] H. Zeng, L. Deng, K. Yang, B. Huang, H. Zhang, Z. Shi, W. Zhang, Degradation of sulfamethoxazole using peroxymonosulfate activated by self-sacrificed synthesized CoAl-LDH@CoFe-PBA nanosheet: Reactive oxygen species generation routes at acidic and alkaline pH, Sep. Purif. Technol. 268 (2021), https://doi.org/10.1016/j.seppur.2021.118654.
[38] B. Gao, S. Zhu, J. Gu, Y. Liu, X. Yi, H. Zhou, Superoxide radical mediated Mn(III) formation is the key process in the activation of peroxymonosulfate (PMS) by Mn-incorporated bacterial-derived biochar, J. Hazard. Mater. 431 (2022), 128549, https://doi.org/10.1016/j.jhazmat.2022.128549.
[39] E.T. Yun, J.H. Lee, J. Kim, H.D. Park, J. Lee, Identifying the nonradical mechanism in the peroxymonosulfate activation process: singlet oxygenation versus mediated electron transfer, Environ. Sci. Technol. 52 (2018) 7032–7042, https://doi.org/10.1021/acs.est.8b00959.
[40] C. Li, J. Wu, W. Peng, Z. Fang, J. Liu, Peroxymonosulfate activation for efficient sulfamethoxazole degradation by Fe3O4/B-FeOOH nanocomposites: coexistence of radical and non-radical reactions, Chem. Eng. J. 356 (2019) 904–914, https://doi.org/10.1016/j.cej.2018.09.064.
[41] C. Richard, J. Lemaire, Analytical and kinetic study of the phototransformation of furfuryl alcohol in aqueous ZnO suspensions, 1990.
[42] S. Deo, W. Medlin, E. Nikolla, M.J. Janik, Reaction paths for hydrodeoxygenation of furfuryl alcohol at TiO2/Pd interfaces, J. Catal. 377 (2019) 28–40, https://doi.org/10.1016/j.jcat.2019.07.012.
[43] L. Wang, B. Li, D.D. Dionysiou, B. Chen, J. Yang, J. Li, Overlooked formation of $H_2O_2$ during the hydroxyl radical-scavenging process when using alcohols as scavengers, Environ. Sci. Technol. 56 (2022) 3386–3396, https://doi.org/10.1021/acs.est.1c03796.
[44] N.T.H. Le, J. Ju, B. Kim, M.S. Kim, C. Lee, S. Kim, W. Choi, K. Kim, J. Kim, Freezing-enhanced non-radical oxidation of organic pollutants by peroxymonosulfate, Chem. Eng. J. 388 (2020), https://doi.org/10.1016/j.cej.2020.124226.
[45] Y. Yang, G. Banerjee, G.W. Brudvig, J.H. Kim, J.J. Pignatello, Oxidation of organic compounds in water by unactivated peroxymonosulfate, Environ. Sci. Technol. 52 (2018) 5911–5919, https://doi.org/10.1021/acs.est.8b00735.
[46] K. Villa, S. Murcia-López, T. Andreu, J.R. Morante, Mesoporous WO3 photocatalyst for the partial oxidation of methane to methanol using electron scavengers, Appl. Catal. B: Environ. 163 (2015) 150–155, https://doi.org/10.1016/j.apcatb.2014.07.055.
[47] D. Xia, H. He, H. Liu, Y. Wang, Q. Zhang, Y. Li, A. Lu, C. He, P.K. Wong, Persulfate-mediated catalytic and photocatalytic bacterial inactivation by magnetic natural ilmenite, Appl. Catal. B: Environ. 238 (2018) 70–81, https://doi.org/10.1016/j.apcatb.2018.07.003.
[48] J. Rodríguez-Chueca, C. Amor, T. Silva, D.D. Dionysiou, G. Li Puma, M.S. Lucas, J. A. Peres, Treatment of winery wastewater by sulphate radicals: HSO5−/transition

metal/UV-A LEDs, Chem. Eng. J. 310 (2017) 473–483, https://doi.org/10.1016/j.cej.2016.04.135.
[49] H. Sun, G. Li, X. Nie, H. Shi, P.K. Wong, H. Zhao, T. An, Systematic approach to in-depth understanding of photoelectrocatalytic bacterial inactivation mechanisms by tracking the decomposed building blocks, Environ. Sci. Technol. 48 (2014) 9412–9419, https://doi.org/10.1021/es502471h.
[50] R. Xiao, K. Liu, L. Bai, D. Minakata, Y. Seo, R. Kaya Göktaş, D.D. Dionysiou, C. J. Tang, Z. Wei, R. Spinney, Inactivation of pathogenic microorganisms by sulfate radical: Present and future, Chem. Eng. J. 371 (2019) 222–232, https://doi.org/10.1016/j.cej.2019.03.296.
[51] A.R. Lado Ribeiro, N.F.F. Moreira, G. Li Puma, A.M.T. Silva, Impact of water matrix on the removal of micropollutants by advanced oxidation technologies, Chem. Eng. J. 363 (2019) 155–173, https://doi.org/10.1016/j.cej.2019.01.080.
[52] P. Garcia-Muñoz, W. Dachtler, B. Altmayer, R. Schulz, D. Robert, F. Seitz, R. Rosenfeldt, N. Keller, Reaction pathways, kinetics and toxicity assessment during the photocatalytic degradation of glyphosate and myclobutanil pesticides: Influence of the aqueous matrix, Chem. Eng. J. 384 (2020), 123315, https://doi.org/10.1016/j.cej.2019.123315.
[53] I. García-Fernández, S. Miralles-Cuevas, I. Oller, S. Malato, P. Fernández-Ibáñez, M. I. Polo-López, Inactivation of E. coli and E. faecalis by solar photo-Fenton with EDDS complex at neutral pH in municipal wastewater effluents, J. Hazard. Mater. 372 (2019) 85–93, https://doi.org/10.1016/j.jhazmat.2018.07.037.
[54] K. Liu, L. Bai, Y. Shi, Z. Wei, R. Spinney, R.K. Göktaş, D.D. Dionysiou, R. Xiao, Simultaneous disinfection of E. faecalis and degradation of carbamazepine by sulfate radicals: an experimental and modelling study, Environ. Pollut. 263 (2020), 114558, https://doi.org/10.1016/j.envpol.2020.114558.
[55] L.C.C. Ferreira, M. Castro-Alférez, S. Nahim-Granados, M.I.I. Polo-López, M.S. S. Lucas, G. Li Puma, P. Fernández-Ibáñez, Inactivation of water pathogens with solar photo-activated persulfate oxidation, Chem. Eng. J. 381 (2020), 122275, https://doi.org/10.1016/j.cej.2019.122275.
[56] D. Venieri, A. Karapa, M. Panagiotopoulou, I. Gounaki, Application of activated persulfate for the inactivation of fecal bacterial indicators in water, J. Environ. Manag. 261 (2020), 110223, https://doi.org/10.1016/j.jenvman.2020.110223.
[57] J. Rodríguez-Chueca, E. Barahona-García, V. Blanco-Gutiérrez, L. Isidoro-García, A.J. dos santos-García, Magnetic CoFe2O4 ferrite for peroxymonosulfate activation for disinfection of wastewater, Chem. Eng. J. 398 (2020), 125606, https://doi.org/10.1016/j.cej.2020.125606.
[58] K. Liu, L. Bai, Y. Shi, Z. Wei, R. Spinney, R.K. Göktaş, D.D. Dionysiou, R. Xiao, Simultaneous disinfection of E. faecalis and degradation of carbamazepine by sulfate radicals: an experimental and modelling study, Environ. Pollut. 263 (2020), https://doi.org/10.1016/j.envpol.2020.114558.
[59] I. Berruti, M. Inmaculada Polo-López, I. Oller, J. Flores, M. Luisa Marin, F. Bosca, Sulfate radical anion: laser flash photolysis study and application in water disinfection and decontamination, Appl. Catal. B: Environ. 315 (2022), 121519, https://doi.org/10.1016/j.apcatb.2022.121519.
[60] S. Mohammadi, G. Moussavi, S. Shekoohiyan, M.L. Marín, F. Boscá, S. Giannakis, A continuous-flow catalytic process with natural hematite-alginate beads for effective water decontamination and disinfection: peroxymonosulfate activation leading to dominant sulfate radical and minor non-radical pathways, Chem. Eng. J. 411 (2021), https://doi.org/10.1016/j.cej.2020.127738.
[61] R. Xiao, L. Bai, K. Liu, Y. Shi, D. Minakata, C.H. Huang, R. Spinney, R. Seth, D. D. Dionysiou, Z. Wei, P. Sun, Elucidating sulfate radical-mediated disinfection profiles and mechanisms of Escherichia coli and Enterococcus faecalis in municipal wastewater, Water Res. 173 (2020), 115552, https://doi.org/10.1016/j.watres.2020.115552.